Ammonia-Mediated CO_2 Capture and Direct Electroreduction to Formate

Hengzhou Liu[a], Yifu Chen[a], Jungkuk Lee[a], Shuang Gu[b], and Wenzhen Li[a]*

Corresponding author: wzli@iastate.edu

a. Department of Chemical and Biological Engineering, Iowa State University, Ames, Iowa 50011, United States

b. Department of Mechanical Engineering, Wichita State University, Wichita, Kansas 67260, United States

*Corresponding author: wzli@iastate.edu

Experimental section:

1. Preparation of electrodes

The electrodeposited-Bi (ED-Bi) was prepared in a two-electrode system in a one-compartment electrochemical cell by a modified method from literature.[1] The aqueous Bi^{3+} precursor was prepared by adding 1.5 mmol of $Bi(NO_3)_3{\cdot}5H_2O$ into 40 mL of deionized water. Concentrated HNO_3 (5 mL) was added to the solution in order to fully dissolve the Bi precursor. The electrodeposition was conducted at a constant current of 72 mA for 5 min. A piece of carbon paper (3 × 3 cm^2, Freudenberg H23) and Pt foil were immersed in the electrolyte as cathode and anode, respectively.

2. Materials characterization

X-ray diffraction (XRD) crystallography was collected with a Siemens D500 diffractometer operated with a Copper K-α source (λ = 1.5418 Å) at 45 kV and 30 mA and equipped with a diffracted beam monochromator (carbon). Scanning Electron Microscopy (SEM) was conducted on a field-emission scanning electron microscope (FEI Quanta-250) equipped with a light-element X-ray detector and an Oxford Aztec energy-dispersive X-ray analysis system.

3. Electrochemical measurements

3.1. Electrochemical conversion of CO_2 captured solutions in the flow cell

The flow electrolyzer contains two flow-field plates with serpentine channels, PTFE and silicone gaskets, and the MEA, which contains two electrodes and a membrane, and was formed after assembling the cell hardware. The anode (2.5 × 2.5 cm^2) and cathode (2.0 × 2.0 cm^2) flow plates were made from titanium and stainless steel, respectively. The catholyte and anolyte were circulated by a peristaltic pump (Masterflex® L/S®) at 50 mL min^{-1}. A piece of Ni foam (MTI corporation, 80–110 pores per Inch, average hole diameters about 0.25 mm) with geometric area of 6.25 cm^2 (2.5 × 2.5 cm^2) and 40 mL of 1.0 M KOH were used as the anode and anolyte, respectively. The prepared ED-Bi on carbon paper and a 2.5 M of CO_2-capturing solution (*i.e.*, NH_4HCO_3, $KHCO_3$, or MEA-CO_2) were used as the cathode and catholyte, respectively. The volume of catholyte was 40 mL and 120 mL for the current density of 100–150 mA cm^{-2} and 200–300 mA cm^{-2}, respectively. A piece of bipolar membrane (Fumatech FBM), anion-exchange membrane (Tokuyama A201), or cation exchange membrane (Nafion115) was used as the ion exchange membrane. Argon was purged into the headspace of the catholyte for the on-line collection and off-line quantification of gaseous products (CO, H_2, and CO_2). The temperature of the flow cell was controlled by a 50-watt 110 V heater (Dioxide Materials).

The 5-hour electrolysis was performed in a similar flow cell set-up with an anion-exchange membrane (Tokuyama A201). The photo of the experimental set-up is shown in **Figure S3**. The volumes of catholyte and anolyte were 500 and 200 mL, respectively. The headspace of catholyte was directly connected to an NH_3 absorbing solution (0.2 M H_2SO_4, 200 mL). The formate concentration in both catholyte and anolyte was quantified by NMR spectroscopy at each hour interval, and the total absorbed NH_4^+ in the absorbing solution was quantified after electrolysis.

3.2. Production of NH_4HCO_3 from CO_2 and nitrate (NO_3^-)-derived NH_3

The experimental setup for NH_4HCO_3 production consists of two major components connected in tandem (**Figure S5**): an electrolyzer for NH_3 production by NO_3^- electro-reduction, and an NH_4HCO_3 formation unit for the reaction between NH_3 and CO_2. The configuration of the one-compartment NH_3-producing electrolyzer was modified from our previous work.[2] In brief, the cell body consisted of a 100 mL screw-cap polytetrafluoroethylene (PTFE) bottle and a custom-made stainless-steel lid. The electrolyte contained 29.7 g of NaOH, 48.1 g of KOH, and 38.9 g of deionized water (with 60wt.% base with equimolar NaOH and KOH, and 40wt.% of H_2O). 139.9 mmol of KNO_3 was added as the reactant. The cell was kept at 80 °C in an oil bath. Two 10 cm^2 nickel mesh electrodes (3.3 × 3 cm^2, 200 mesh) attached to nickel wires (0.04" diameter) were used as the cathode and anode, and a flow of N_2 (200 mL min^{-1}) was bubbled into the electrolyte to carry the produced NH_3 into the NH_4HCO_3 formation unit, which consisted of 100 mL of

CO_2-saturated deionized water cooled to 5 °C and magnetically stirred at 400 r.p.m. To maintain the saturation of CO_2, 500 mL min^{-1} of CO_2 was bubbled into the NH_4HCO_3 formation unit during the experiment. Electrolysis was carried out at a constant current density of 500 mA cm^{-2} for 6 hours; under these conditions, the applied charge was equal to the theoretical amount of charge required to fully reduce NO_3^- in the system to NH_3. To determine the utilization of NH_3 in the NH_4HCO_3 formation unit, the outlet gas from the NH_4HCO_3 formation unit was bubbled into an acidic solution (100 mL of 0.5 M H_2SO_4) to collect any unused NH_3.

To obtain solid NH_4HCO_3 sample for further *i*-CO2RR experiments, a similar configuration with larger electrolyzer volume (2.5 L) was used with 25 times the quantity of all chemicals for electrolyte preparation. The detailed description of the scaled-up electrolyzer and its ammonia-production performances are reported in Ref 50 (main article). Other conditions include: 2.8 mol of added KNO_3 as the reactant, 100 cm^2 of the electrode area, 500 mL min^{-1} of the N_2 flow rate, 250 mA cm^{-2} of the applied current density, and 24 hours of the electrolysis duration. Due to the low solubility of NH_4HCO_3 (1.81 mol per liter of water at 5 °C), solid was precipitated in the NH_4HCO_3 formation unit, which was separated by vacuum filtration. The effective NH_4HCO_3 content of the collected sample was determined by dissolving a certain amount of the sample in deionized water, followed by measuring its NH_4^+ concentration (detailed in the following section).

4. Product analysis

4.1. Quantification of soluble products in the electrolyte

Formate was quantified by an ion chromatography (IC, Thermo Scientific Dionex Easion). 50 or 100 μL of the sample solution was diluted with deionized water and injected into IC for its quantification.

NO_3^- and NO_2^- were analyzed by High-Performance Liquid Chromatography (HPLC)[3] (Agilent Technologies, 1260 Infinity II LC System) equipped with a variable wavelength detector (Agilent 1260 Infinity Variable Wavelength Detector VL). The wavelength of 213 nm was used for detection. A C18 HPLC column (Gemini® 3 μm, 110 Å, 100 × 3 mm) was used for analysis at 25 °C with a binary gradient pumping method to drive mobile phase at 0.4 mL min^{-1}. The mobile phase consisted of 0.01 M *n*-octylamine (for ion pairing) in a mixed solution containing 30 vol% of methanol and 70 vol% of DI water, and the pH of the mobile phase was adjusted to 7.0 with H_3PO_4. The running time was 30 min for each sample, and the retention time for NO_3^- and NO_2^- was around 18 and 16 min, respectively. The calibration solutions for NO_3^- or NO_2^- were prepared with KNO_3 and KNO_2 in the concentration range of 0.0625–2 mM.

For the electrochemical NO_3^--to-NH_3 reaction, the conversion of NO_3^- (X) and faradaic efficiency of product i (FE_i for NH_3 and NO_2^-) were calculated by

$$X = \frac{n_0 - n}{n_0} \times 100\%$$

$$\mathrm{FE}_i = \frac{n_i \cdot z_i \cdot F}{Q} \times 100\%$$

where n_0 is the initial amount of NO_3^- (mol); n is the amount of NO_3^- after electrolysis (mol); n_i is the amount of product i (mol); z_i is the number of electrons transferred to product i; F is the Faraday constant (96,485 C mol^{-1}); Q is the total charge passed through the electrolytic cell (C).

NH_4^+ content was determined by ^1H Nuclear Magnetic Resonance (NMR) spectroscopy on a Bruker Avance NEO 400 MHz NMR spectrometer. The sample solution was first diluted with 0.1 M H_2SO_4 to the proper range of NH_3 concentration. 800 μL of the diluted sample solution was then mixed with 200 μL of DMSO-d_6 and 200 μL of 32 μM maleic acid (internal standard) in DMSO-d_6. The scan number was 1,024 with a water suppression method. Standard NH_3 solutions were prepared for calibration with concentrations ranging from 0 to 5 mg L^{-1} (in N).

4.2. Quantification of gas products

The gas products were analyzed by an off-line gas chromatography (GC, SRI Instruments, 8610C, Multiple Gas #3) equipped with HayeSep D and MolSieve 5Å columns. A thermal conductivity detector was used to detect H_2, and a flame ionization detector was used to detect CO and CO_2. The calibration curves for H_2 (10–10,000 ppm, Cal Gas Direct), CO (110–8,000 ppm, Cal Gas Direct), and CO_2 (5,000 – 50,000 ppm, Cal Gas Direct) were established by analyzing the calibration gases.

In the electrolysis of CO_2-capturing solutions at 5 min, 15 min, and 25 min, the outlet of the electrolyzer was connected to a standard FlexFoil sample bag (1 L, SKC INC) for on-line collection of gas products. Then, the collected gases were injected into GC for their off-line analysis. A 12-min GC program was applied. The rate of gas generation (r, mol s^{-1}) was calculated by

$$r = c \times 10^{-6} \times \frac{p\dot{V} \times 10^{-6} / 60}{RT}$$

where c is the gas content (ppm); $\dot{V}$ is the volumetric flow rate of the inlet gas to the sample bags (300 mL min^{-1}); p is the atmospheric pressure (1.013×10^5 Pa); R is the gas constant (8.314 J mol^{-1} K^{-1}); T is the room temperature (20 °C or 293.15 K). The total amount of gas production (mol) was calculated by integrating the plot of gas production rate (mol s^{-1}) *vs.* reaction time (s) with a linear fitting.

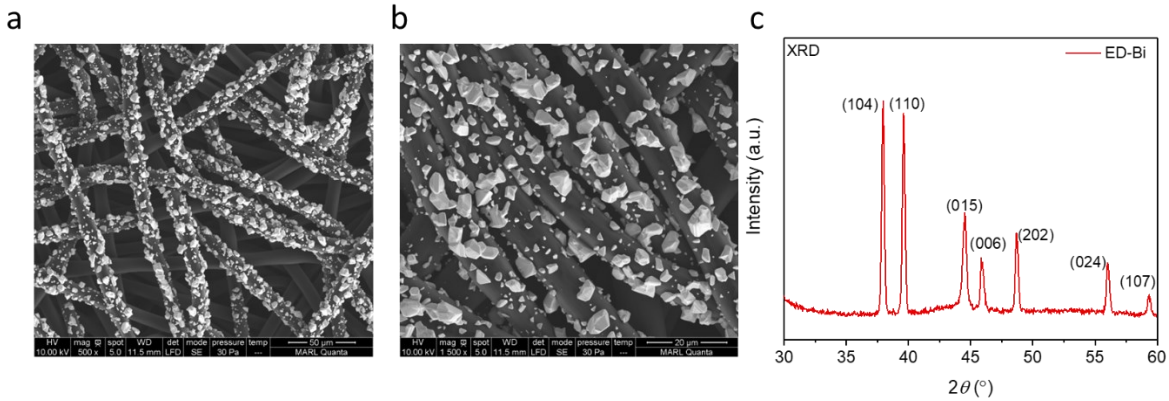

Figure S1. Characterization of ED-Bi. (a) SEM image (scale bar = 50 μm), (b) SEM image with higher magnification (scale bar = 20 μm), and (c) XRD pattern of ED-Bi.

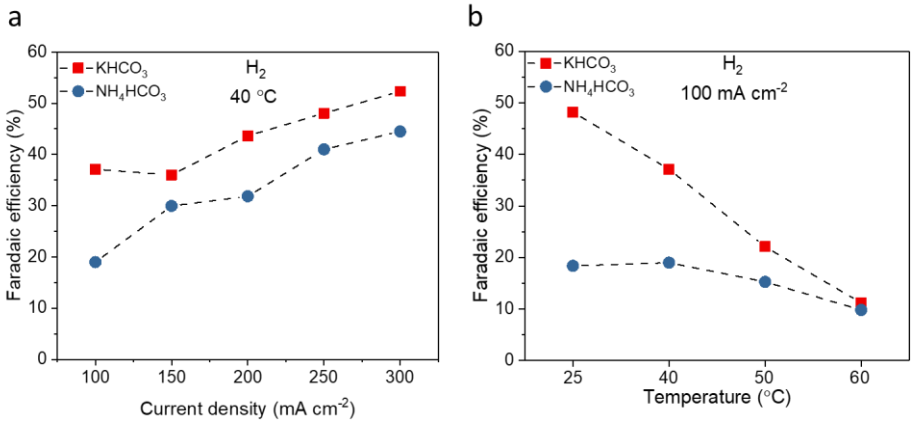

Figure S2. Comparison of H_2 faradaic efficiency between $KHCO_3$ and NH_4HCO_3 at (a) different current densities and (b) different cell temperatures for BPM-based electrolysis for half-hour operation. The catholyte volume was 120 mL for 200–300 mA cm^{-2} and 40 mL for 100–150 mA cm^{-2}.

Table S1. The source of *i*-CO_2 in the BPM-based electrolyzers with $KHCO_3$ or NH_4HCO_3 at cell temperature of 40 °C for half-hour operation.

System	Total *i*-CO_2 (mmol)[a]	*i*-CO_2 from thermal decomposition (mmol)[b]	*i*-CO_2 from BPM-induced chemical decomposition (mmol)[c]
$KHCO_3$	4.2	2.2	2.0
NH_4HCO_3	14.1	12.5	1.6

a. Total *i*-CO_2 values were obtained by summing the amounts of both unreacted CO_2 and reacted CO_2 (or generated *i*-CO2RR products) at the cathode during the half-hour electrolysis.
b. The values of *i*-CO_2 from thermal decomposition were experimentally obtained (by online GC) from the same BPM-based electrolyzer without applying any current.
c. The *i*-CO_2 values from BPM-induced chemical decomposition were obtained from subtracting the "*i*-CO_2 from thermal decomposition" from the "total *i*-CO_2".

Table S2. Summary of the faradaic efficiencies of *i*-CO_2 reduction products in the BPM-based electrolyzers with $KHCO_3$ or NH_4HCO_3 at different reaction conditions.

Conditions		FE towards H_2 (%)	FE towards formate (%)	FE towards CO (%)	Total (%)
$KHCO_3$ (40 °C)	100 mA/cm^2	37.11	59.50	1.96	**98.57**
	150 mA/cm^2	36.02	60.00	1.74	**97.76**
	200 mA/cm^2	43.64	56.64	1.81	**102.09**
	250 mA/cm^2	48.04	51.88	1.57	**101.49**
	300 mA/cm^2	52.32	46.93	1.50	**100.75**
NH_4HCO_3 (40 °C)	100 mA/cm^2	18.98	79.49	3.45	**101.92**
	150 mA/cm^2	29.96	69.33	2.76	**102.05**
	200 mA/cm^2	31.84	69.83	3.00	**104.67**
	250 mA/cm^2	41.00	59.16	2.06	**102.22**
	300 mA/cm^2	44.50	54.81	2.39	**101.70**
$KHCO_3$ (100 mA cm^{-2})	RT (25 °C)	48.18	54.99	2.06	**105.23**
	50 °C	22.10	74.50	2.79	**99.39**
	60 °C	11.20	82.11	3.36	**96.67**
NH_4HCO_3 (100 mA cm^{-2})	RT (25 °C)	18.37	76.92	2.60	**97.89**
	50 °C	15.26	82.58	3.72	**101.56**
	60 °C	9.81	89.00	4.08	**102.89**

Table S3. The detection of crossover in the NH_4HCO_3 systems with three membranes.[a]

System	Formate in Catholyte (mM)	Formate in anolyte (mM)	Crossover percentage (%)
BPM	74.13	None	0
CEM	61.99	None	0
AEM	75.21	3.75	4.7

a. The electrolysis was performed at 100 mA cm^{-2} for half-hour.

Supporting Information Note 1, Corrosiveness and Toxicity Comparison between Ammonia and KOH

Ammonia is less corrosive and less toxic than KOH. The detailed comparisons between ammonia and KOH in terms of corrosiveness and toxicity are drawn as follows.

(1) Corrosiveness: NH_3 is **less** corrosive than alkali metal hydroxides (NaOH, KOH) and amines in aqueous solutions, as shown in **Table 1** of the **Ref.** (*Applied Energy,2018,* 230, 734-749)[4]. This is consistent with the pH difference: the pH is lower for ammonium hydroxide (pH = 11.3) than for KOH (pH = 13) at the same concentration of 0.1 M in water (https://scrippslabs.com/ph-of-common-reagents-at-room-temperature/)

(2) Toxicity: ammonia (ammonium hydroxide) is **less** toxic than KOH: The lethal dose (LD_{50}) is about 30% higher for ammonium hydroxide than for KOH.

LD_{50} (ammonium hydroxide) = ~350 mg/kg-rat (https://www.tannerind.com/PDF/Ammonium-Hydroxide-SDS.pdf);

LD_{50} (KOH) = 273 mg/kg-rat (https://fscimage.fishersci.com/msds/19431.htm)

The future scale-up of NH_3-mediated CO_2 capture and its reduction will require the rational design of reactors to address corrosion concerns. The toxicity of NH_3 should also require the cautious operation of NH_3-based solutions or gases. Despite its toxicity and corrosiveness, NH_3 is easily stored and transported with a proven acceptable safety history for over 80 years. With the mature protocols for professional NH_3 handling in place, its risk should be largely mitigated[5]. Therefore, no significant effort is expected to scale up or deploy the ammonia-assisted CO_2 capture for practical applications.

Supporting Information Note 2, Ammonia Loss Analysis

The pH of our cathode electrolyte and the dominance of NH_4^+: Our system (2.5 M NH_4HCO_3) has a mild and stable alkalinity, pH = 7.8, which can be seen in the Handbooks in Separation Science – Capillary Electromigration Separation Methods.[6] The pH of NH_4HCO_3 aqueous solutions is in the middle of the pKa of NH_4^+ (9.26) and pKa of HCO_3^- (6.35). Therefore, NH_4^+ is indeed the dominating species (96.6% of all nitrogen at 25 °C) in the NH_4^+(aq)/NH_3(aq) equilibrium.

The two equilibria: One is the NH_3(g)/NH_3(aq) equilibrium, and the other is the NH_4^+(aq)/NH_3(aq) equilibrium. The two equilibria are independent and subject to different equilibrium constants: The first is governed by the Henry's law, and the second is controlled by the solution pH. In our cathode electrolyte (2.5 M NH_4HCO_3), the maximum partial pressure of NH_3(gas) on the immediate surface of the solution is merely 98.6 Pa (or ~0.1vol.%), based on the Henry's constant at 25 °C [69 mol/(kg·bar) in NIST Chemistry WebBook[7]]. NH_3 loss was not observed in our experiments using 2.5 M NH_4HCO_3.

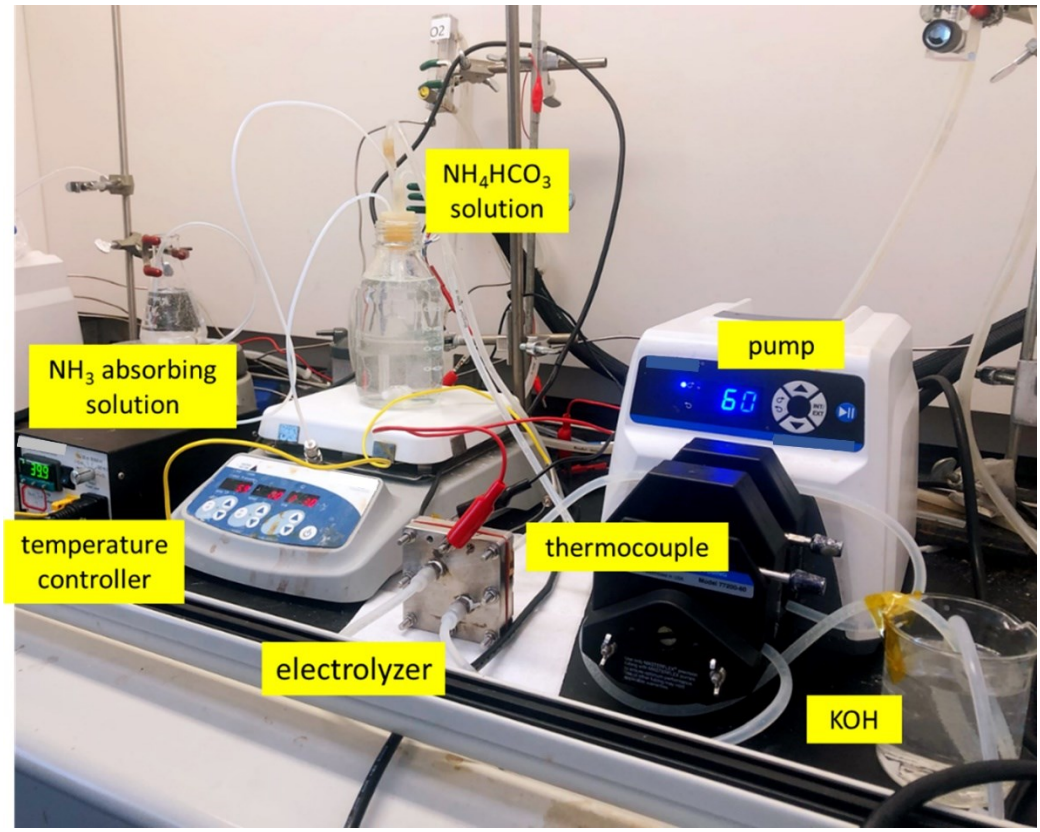

Figure S3. Photograph of the experimental system for the 5-hour electrolysis of NH_4HCO_3 in the AEM-based electrolyzer. Credits:

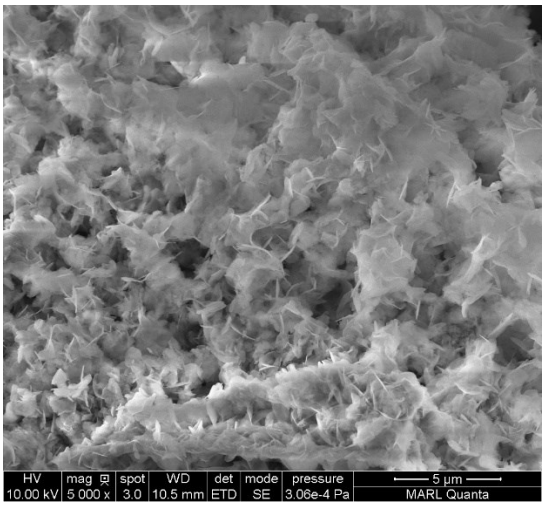

Figure S4. SEM image of ED-Bi after 5-hour electrolysis.

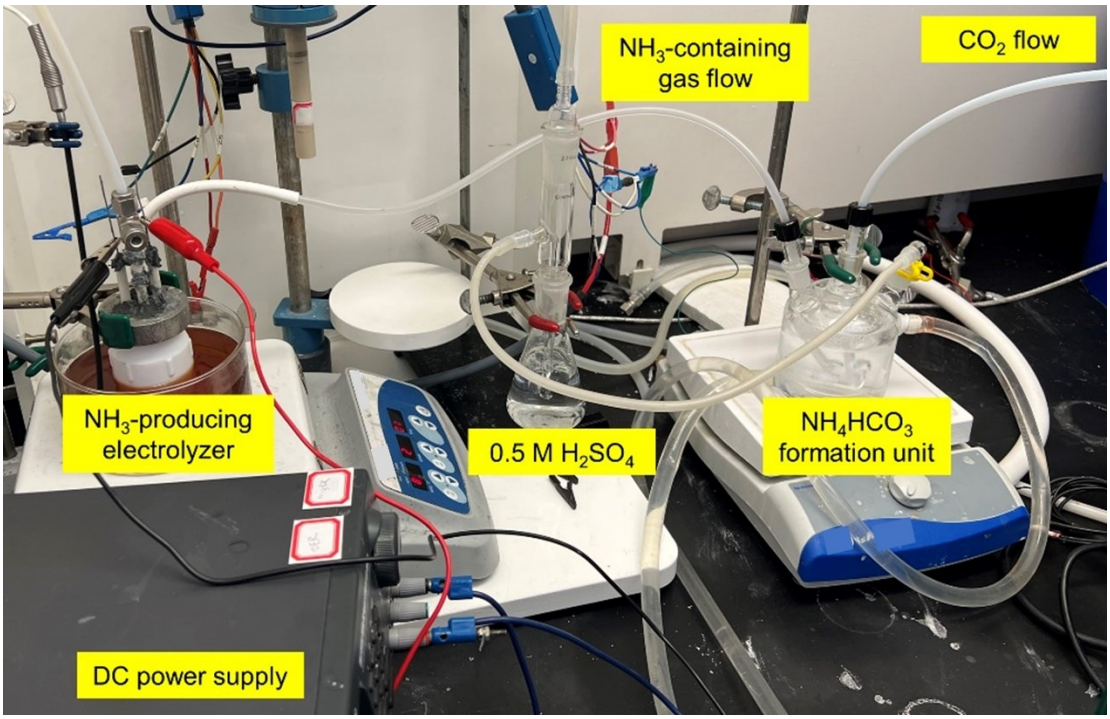

Figure S5. Photograph of the experimental system for the production of NH_4HCO_3 from CO_2 and NO_3^--derived NH_3.

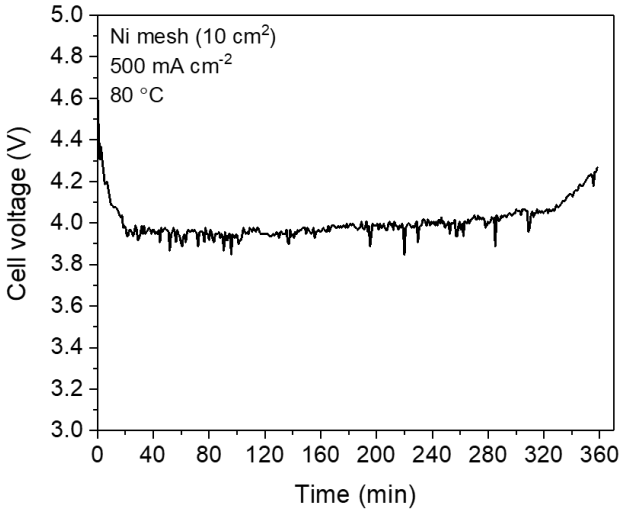

Figure S6. Cell voltage profile of NH_3 production by NO_3^- reduction in the alkaline electrolyzer for 6-hour electrolysis.

Supporting Information Note 3, Energy Consumption Estimation

We calculated the energy consumption for CO_2 reduction toward formate in different well-known cell configurations:

(1) Feed pure CO_2 gas:

(1-i) gas and liquid feed-alkaline flow electrolyzer

(1-ii) gas-feed membrane electrode assembly flow electrolyzer

(2) Feed CO_2 capture solutions:

(2-i) $KHCO_3$ feed into bipolar membrane (BPM)-based electrolyzer

(2-ii) MEA-CO_2 feed into BPM-based electrolyzer

(2-iii) NH_4HCO_3 feed into BPM-based electrolyzer

(2-iv) NH_4HCO_3 feed into cation exchange membrane (CEM)-based electrolyzer

(2-v) NH_4HCO_3 feed into anion exchange membrane (AEM)-based electrolyzer

HER was assumed as the only side reaction. The current density was assumed at 100 mA cm^{-2}.

CO_2 regeneration. In the conventional cases by feeding purified CO_2, significant energy input is required to regenerate CO_2 through a few thermal and compression steps.[8, 9] From a typical calcium caustic recovery loop, the energy consumption for CO_2 regeneration ($CaCO_3 \rightarrow CaO + CO_2$) is 178.3 kJ/mol_{CO2}.[8]

In the alkaline electrolyzer (i-1), the major loss of CO_2 could be due to the combination (or alkaline hydration) reaction ($CO_2 + OH^- \rightarrow HCO_3^-$) and the crossover of bicarbonate from the cathode to the anode. Based on the previous literature,[10, 11] a model can be built to estimate the CO_2 consumption. At the steady state, the rate of CO_2 supply (through diffusion) is equal to that of CO_2 combination reaction in the nearby region of the cathode:

$$D_{\mathrm{CO2}} \frac{\mathrm{d}^2 c}{\mathrm{d}x^2} = k \cdot c \cdot [\mathrm{OH}^-]$$

where D_{CO2} is the diffusion coefficient of CO_2 in water (1.91×10^{-9} $m^2 \cdot s^{-1}$), c is the CO_2 concentration in electrolyte (M), x (m) is the distance between an electrolyte location and the gas-solution interface, k is the rate constant for the combination reaction ($CO_2 + OH^- \rightarrow HCO_3^-$, 2.23 $mol^{-1} \cdot m^3 \cdot s^{-1}$), and $[OH^-]$ is the concentration of OH^- (a constant 1 M assumed in this work). Solving the equation by integration and considering the boundary conditions ($c = c_0$, or interfacial CO_2 concentration, when $x = 0$; and $c = 0$, when $x = +\infty$), the following expression can be obtained:

$$c = c_0 \cdot \exp\left(-\sqrt{\frac{k[\mathrm{OH}^-]}{D_{\mathrm{CO2}}}} \cdot x\right)$$

where c_0 is the interfacial CO_2 concentration in the electrolyte at the gas-solution interface, which is assumed as the CO_2 solubility (0.038 M understand the standard conditions) in water. The CO_2 consumption rate due to the combination reaction (J_h), which is the flux of CO_2 across the gas-solution interface, is calculated, as follows:

$$J_h = -D_{CO2} \cdot \frac{dc}{dx}|_{x=0} = c_0 \cdot \sqrt{k \cdot D_{CO2} \cdot [OH^-]} = 7.84 \times 10^{-6}\ \text{mol} \cdot \text{s}^{-1} \cdot \text{cm}^{-2}$$

The CO_2 consumption due to its reduction reaction at 100 mA cm^{-2} is calculated, as follows:

$$J_r = \frac{n \cdot j_{CO2}}{z \cdot F} = \frac{1 \cdot 0.1}{2 \cdot 96485} = 5.18 \times 10^{-7}\ \text{mol} \cdot \text{s}^{-1} \cdot \text{cm}^{-2}$$

where j_{CO2} is the partial current density of CO_2 reduction, n is the number of required CO_2 molecules for one molecular formate produced (n = 1 here), z is the number of electrons involved in the CO_2-to-formate reaction, and F is the Faraday constant (96,485 C·mol^{-1}).

Then, the CO_2 utilization in the alkaline electrolyzer (1-i) is calculated, as follows:

CO_2 utilization = $J_r/(J_r + J_h)$ = 6.2%

Membrane electrode assembly-based flow electrolyzers by using AEM suffer from a ~30% CO_2 loss due to the bicarbonate crossover from cathode to anode,[12, 13] regardless of feeding with either a humidified pure CO_2 gas (1-ii) or circulating aqueous NH_4HCO_3 (2-v). In addition, when feeding pure CO_2 into the MEA cell, there is an additional ~35% CO_2 loss due to the escape of unreacted CO_2.[13] As such, the CO_2 utilization in the MEA-based electrolyzers with AEM can be estimated as 35% and 70% when feeding gaseous CO_2 and aqueous NH_4HCO_3, respectively.

By contrast, 90% of CO_2 utilization can be assumed for the cases of using BPM or CEM when feeding CO_2 capture solutions (2-i, 2-ii, 2-iii, and 2-iv), by avoiding the bicarbonate crossover between electrodes and the gas escape at cathode.[13, 14]

Table S4. Summary of CO_2 consumption and utilization for all cases.

	CO_2 consumption				Total CO_2 utilization
Case	Combination reaction	HCO_3^- crossover	Unreacted escape	Total	
1-i	93.8%			93.8%	6.2%
1-ii		30%	35%	65%	35%
2-i				0%	90%
2-ii				0%	90%
2-iii				0%	90%
2-iv				0%	90%
2-v		30%		30%	70%

Thus, the energy consumption for CO_2 regeneration is shown as follows:

CO_2 regeneration energy = (178.3 kJ/mol) / (CO_2 utilization)

Thermodynamic energy

In the AEM-based eletrolyzer through NH_4HCO_3 feed (case 2-v), the cathodic electrolyte is 2.5 M NH_4HCO_3, and the anodic electrolyte is 1 M KOH. An AEM separates the cathodic and anodic electrolytes.

1. Estimation of catholyte pH during electrolysis

   The catholyte is 40 mL of 2.5 M NH_4HCO_3 and acts as a buffer. The total amount of NH_4HCO_3 before thermodynamic equilibrium is 40 × 2.5 = 100 mmol. At the equilibrium, the pH of the 2.5 M NH_4HCO_3 is ~7.80 (*i.e.*, the middle point between the two p*K*a values: 6.35 of H_2CO_3 and 9.25 of NH_4^+, CRC handbook). Therefore, the amounts of NH_4^+ and NH_3 are 96.45 mmol (96.45% of N) and 3.55 mmol (3.55% of N), respectively, based on the Henderson-Hasselbalch equation: $pH = pK_a(NH_4^+) + \log_{10}([NH_3]/[NH_4^+])$ and the mass conservation ($[NH_3] + [NH_4^+] = 100$ mmol), where $[NH_3]$ and $[NH_4^+]$ are concentrations of NH_3 and NH_4^+, respectively.

   The cathodic reaction is

   $CO_2 + 2e^- + H_2O \rightarrow HCOO^- + OH^-$

   After electrolysis at 400 mA (100 mA cm^{-2}) for 30 min, the cathodic reaction generates 3.7 mmol of OH^- (assuming 100% FE to $HCOO^-$), and this OH^- should react with and thus turn 3.7 mmol NH_4^+ to NH_3. Based on the measurement of *i*-CO_2, the total decomposed NH_4HCO_3 should be 14.1 mmol. So, the remaining NH_4^+ is 96.45 – 3.7 – 14.1 × 96.45% = 79.15 mmol. The amount of remaining NH_3 is 3.55 + 3.7 – 14.1 × 3.55% = 6.75 mmol.

   Using the Henderson-Hasselbalch equation, the solution pH after electrolysis reaction is

   $pH = pK_a(NH_4^+) + \log_{10}([NH_3]/NH_4^+]) = 9.25 + \log_{10}(6.75/79.15) = 8.18$

   So, we may assume the electrolyte pH is around 8.0 during the reaction. Note that we did not consider the transport of OH^- through the AEM, because the concentration of HCO_3^- is much higher than OH^-.

2. Obtaining the standard reduction potential of $CO_2/HCOO^-$ at pH = 8.0

   From CRC handbook, the following ΔG^0 values can be found:

   ΔG^0 ($HCOO^-$) = –351.0 kJ/mol, ΔG^0 (OH^-) = –157.2 kJ/mol, ΔG^0 (CO_2, gas) = –394.4 kJ/mol, and ΔG^0 (H_2O) = –237.1 kJ/mol

   The cathodic reaction is

   $CO_2 + 2e^- + H_2O \rightarrow HCOO^- + OH^-$

   For this reaction, $\Delta G^0 = -351.0 - 157.2 - (-394.4) - (-237.1) = 123.3$ kJ/mol

   $\varphi^{rev}(CO_2/HCOO^-) = \varphi^0(CO_2/HCOO^-) = -123.3 \times 1000 / (96485 \times 2) = -0.639$ V_{SHE}

   This corresponds to the standard condition at pH = 14 ($[OH^-] = 1$ M). So, the reversible reduction potential at pH = 8.0 is

   $\varphi^{rev}(CO_2/HCOO^-, pH = 8.0) = -0.639 + 0.0592 / (2 \times \log (1 / [OH^-]))$

   $= -0.639 + 0.05916 / (2 \times \log [1 / (10^{-14} / 10^{-8.0})]) = -0.462$ V_{SHE}

3. Obtaining thermodynamic cell voltage for the pH-asymmetric configuration. For clarity, φ^{rev} and E^{rev} are used to stand for the "reversible electrode potential" and the "reversible cell voltage", respectively, throughout this document.

   For the cell with AEM, the cathodic reaction is

$CO_2 + 2e^- + H_2O \rightarrow HCOO^- + OH^-$ (**RXN 1**, pH = 8.0)

The reversible reduction potential for RXN 1 is –0.462 V_{SHE} as we calculated.

And the anodic reaction is

$4OH^- \rightarrow O_2 + 2H_2O + 4e^-$ (**RXN 2**, pH = 14)

The standard reduction potential for RXN 2 is 0.401 V_{SHE} from CRC handbook.

To calculate the thermodynamic cell voltage for the overall reaction, we need to multiply RXN 1 by 2 and add RXN 2 to eliminate the electrons:

$2CO_2 + 4OH^-$ (pH 14) $\rightarrow 2HCOO^- + O_2 + 2OH^-$ (pH 8.0) (**RXN 3**)

Note that OH^- cannot be simply eliminated because of the difference in pH. The thermodynamic cell potential for RXN 3, $\underline{E^{rev}}$ (RXN 3), is –0.462 – 0.401 = –0.863 V

In the actual cell configuration, because AEM can transport OH^-, we should have the following equation:

$2OH^-$ (pH 8.0) $\rightarrow 2OH^-$ (pH 14) (**RXN 4**)

To calculate the reversible potential for this equation, we may use the standard reduction potential of H_2O/H_2:

$2H_2O + 2e^- \rightarrow H_2 + 2OH^-$ (pH 14) (**RXN 5**)

$\varphi^{rev}(H_2O/H_2$, pH 14) = –0.828 V_{SHE} (from CRC handbook)

$2H_2O + 2e^- \rightarrow H_2 + 2OH^-$ (pH 8.0) (**RXN 6**)

$\varphi^{rev}(H_2O/H_2$, pH 8.0) = –0.828 V_{SHE} + 0.05916 / (2 × $\log_{10}(1 / [OH^-]^2)$) = –0.473 V_{SHE}

RXN 4 corresponds to a cell constructed by using RXN 5 as the cathode, and RXN 6 as the anode.

Therefore, E^{rev} for RXN 4 is –0.828 – (–0.473) = –0.355 V

By adding RXN 3 and RXN 4, we have

$2CO_2 + 2OH^-$ (pH 14) $\rightarrow 2HCOO^- + O_2$ (**RXN 7**)

ΔG(RXN 7) = ΔG(RXN 3) + ΔG(RXN 4)

Because $\Delta G = -z \cdot F \cdot \varphi^{rev}$ for reduction electrode reaction or $-z \cdot F \cdot E^{rev}$ for cell reaction, we have

$-4 \times F \times E^{rev}$(RXN 7) = $-4 \times F \times \varphi^{rev}$(RXN 3) – $2 \times F \times E^{rev}$(RXN 4)

E^{rev}(RXN 7) = φ^{rev}(RXN 3) + 1/2 × E^{rev}(RXN 4) = –0.863 + 1/2 × (–0.355) = –1.040 V

So, the thermodynamic cell voltage for RXN 7, E^{rev}(RXN 7), is 1.040 V, which is the thermodynamic cell voltage for our AEM-based electrolyzer.

Note that this value is exactly equal to the cell voltage when we directly calculate the E^{rev} of RXN 7 at standard conditions (pH = 14):

φ^0 ($CO_2/HCOO^-$) = –0.639 V_{SHE} (we calculated this value before)

φ^0 (O_2/OH^-) = 0.401 V_{SHE} (from CRC handbook)

The thermodynamic cell potential E^0 = –0.639 – 0.401 = –1.040 V, corresponding to 1.040 V of thermodynamic cell voltage.

For the CEM electrolyzer (K^+ transport) with NH_3HCO_3 feed (case 2-iv) and BPM electrolyzer with CO_2 capture solutions feed (case 2-i, 2-ii, and 2-iii), the catholyte pH was assumed at 8.0 and anolyte pH was 14.

The thermodynamic cell potential is E^{rev} = –0.462 – 0.401 = –0.863 V, corresponding to thermodynamic cell voltage of 0.863 V.

Considering the different FE of cathodic product (FE_c) in different cell configurations, the actual thermal energy to produce 1 mole of formate product can be calculated as follows:

$$\Delta G_{\text{minimum}} = -z \cdot F \cdot \left(\frac{E^{rev}_{\text{cell-formate}}}{\text{FE}_c}\right)$$

where, z is number of electrons required per mole of formate product; $\Delta G_{\text{minimum}}$ is the required minimum electrical energy applied to the electrolytic cell per unit of formate product, $E_{\text{cell-formate}}°$ is the standard reversible cell voltage for formate production.

From the literature, in the feeding of pure CO_2 (cases 1-i and 1-ii), the FE_c toward target products can attain ~90%.[15, 16] In the feeding of $KHCO_3$ into the BPM-based electrolyzer (case 2-i), as we observed from our experimental results and the literature,[1] the FE_c is assumed as 55%. In the feeding of MEA-CO_2 in the BPM-based electrolyzer (2-ii), the FE_c is assumed as 20% at the current density of 100 mA cm^{-2}. Based on the experimental results, in the feeding of NH_4HCO_3 to AEM (2-v), BPM (2-iii), and CEM (2-iv), the FE_cs are assumed as 90%, 80%, and 70%, respectively.

Table S5. Summary of thermodynamic energy for all cases.

Case	$E^{°}_{\text{cell-formate}}$(V)	FE_c (%)	$\Delta G_{\text{minimum}}$ (kJ mol^{-1})
1-i	–1.040	90	223.0
1-ii	–1.040	90	223.0
2-i	–0.863	55	302.8
2-ii	–0.863	20	832.7
2-iii	–0.863	80	208.2
2-iv	–0.863	70	237.9
2-v	–1.040	90	223.0

Cathode energy loss

Cathode energy loss is due to the overpotential for CO_2 reduction toward target products. Based on the literature, we assumed the overpotential of CO_2-to-formate on Bi-based catalysts at 100 mA cm^{-2} is 0.7 V.[16]

Then, the cathodic energy loss can be calculated, as follows:

Cathode energy loss = $z \cdot F \cdot \eta / \text{FE}_c$

where z is the number of electrons involved in the CO_2-to-formate reaction, and F is the Faraday constant (96,485 C·mol^{-1}).

Anode energy loss

In the alkaline medium (e.g., 1 M KOH), the overpotential for OER on Ni-based catalysts can be as low as < 400 mV at current density of 100 mA cm^{-2}. For example, the literature reported a nanostructured NiCo alloy that shown an overpotential of 326 mV.[17] So, we used this value to calculate anode energy loss, as follows:

Anode energy loss = $z \cdot F \cdot \eta / FE_c = 2 \times 96485 \times 0.326 / FE_c$

where z is the number of electrons involved in the CO_2-to-formate reaction, and F is the Faraday constant (96,485 $C \cdot mol^{-1}$).

Ohmic loss

The Ohmic loss is mainly caused by the membrane resistance.

The potential drop ($\Delta\phi$) across the membrane is calculated as follows:

$$\Delta\phi = \frac{iL}{\kappa}$$

where i is the current density and L is the thickness of the membrane.
Based on the literature, the κ value for AEM (A201 membrane) is around 20 mS cm^{-1} in OH^-.[18] With its thickness of 28 μm and at the current density of 100 mA cm^{-2}, the calculated $\Delta\phi$ is 14 mV.
The κ value for Nafion 115 membrane is 21 mS cm^{-1} in K^+, so the $\Delta\phi$ is 60 mV.

The BPM is thicker than AEM and CEM, because it is sandwiched by a cation exchange layer (CEL) and an anion exchange layer (AEL). The $\Delta\phi$ value for BPM (Fumasep FBM) is assumed to be 280 mV at 100 mA cm^{-2}, based on the specification document.

In addition, 0.828 V potential is required under the standard condition to dissociate water into H^+ and OH^- by using BPM, which should also be included in the ohmic loss.

Therefore, the energy loss due to membrane resistance is calculated as follows:

For AEM and CEM cases: Ohmic loss = $z \cdot F \cdot \Delta\phi / FE_c$

For BPM cases: Ohmic loss = $z \cdot F \cdot (\Delta\phi + 0.828\ V) / FE_c$

Separation of product

In the near neutral media, an electrodialysis (ED) process is used to convert formate to formic acid before the separation of formic acid.[14] Then, a pressure-swing distillation (PSD) method is used for the separation of formic acid from the mixed solutions.[19] The reported energy consumption to separate formic acid is about 265 kJ/mol.[11, 19] The energy consumption in the ED process is ignored in our modeling, because of the much lower energy consumption than the PSD process.[11]

In summary, the total energy consumption can be obtained by summing all components identified above: thermodynamic energy consumption, cathode energy loss, anode energy loss, ohmic energy loss, and separation energy use.

References

1. Li, T.; Lees, E. W.; Zhang, Z.; Berlinguette, C. P., Conversion of bicarbonate to formate in an electrochemical flow reactor. *ACS Energy Letters* **2020,** *5* (8), 2624-2630.
2. Chen, Y.; Liu, H.; Ha, N.; Licht, S.; Gu, S.; Li, W., Revealing nitrogen-containing species in commercial catalysts used for ammonia electrosynthesis. *Nature Catalysis* **2020,** *3* (12), 1055-1061.
3. Chou, S.-S.; Chung, J.; Hwang, D.-F., A high performance liquid chromatography method for determining nitrate and nitrite levels in vegetables. *Journal of Food and Drug Analysis* **2003,** *11* (3), 233-238.
4. Wang, F.; Zhao, J.; Miao, H.; Zhao, J.; Zhang, H.; Yuan, J.; Yan, J., Current status and challenges of the ammonia escape inhibition technologies in ammonia-based CO2 capture process. *Applied Energy* **2018,** *230*, 734-749.
5. Soloveichik, G., Ammonia for energy storage and delivery. *13th Annual NH3 Fuel Conference* **2016**.
6. Poole, C. F., *Capillary Electromigration Separation Methods*. Elsevier: 2018.
7. NIST Chemistry Webbook, SRD69, https://webbook.nist.gov/cgi/cbook.cgi?ID=C7664417&Mask=10
8. Keith, D. W.; Holmes, G.; Angelo, D. S.; Heidel, K., A process for capturing CO2 from the atmosphere. *Joule* **2018,** *2* (8), 1573-1594.
9. Welch, A. J.; Dunn, E.; DuChene, J. S.; Atwater, H. A., Bicarbonate or carbonate processes for coupling carbon dioxide capture and electrochemical conversion. *ACS Energy Letters* **2020,** *5* (3), 940-945.
10. Dinh, C.-T.; Burdyny, T.; Kibria, M. G.; Seifitokaldani, A.; Gabardo, C. M.; García de Arquer, F. P.; Kiani, A.; Edwards, J. P.; De Luna, P.; Bushuyev, O. S., CO2 electroreduction to ethylene via hydroxide-mediated copper catalysis at an abrupt interface. *Science* **2018,** *360* (6390), 783-787.
11. Gu, J.; Liu, S.; Ni, W.; Ren, W.; Haussener, S.; Hu, X., Modulating electric field distribution by alkali cations for CO2 electroreduction in strongly acidic medium. *Nature Catalysis* **2022**, 1-9.
12. Weng, L.-C.; Bell, A. T.; Weber, A. Z., Towards membrane-electrode assembly systems for CO 2 reduction: a modeling study. *Energy & Environmental Science* **2019,** *12* (6), 1950-1968.
13. Lee, G.; Li, Y. C.; Kim, J.-Y.; Peng, T.; Nam, D.-H.; Sedighian Rasouli, A.; Li, F.; Luo, M.; Ip, A. H.; Joo, Y.-C., Electrochemical upgrade of CO2 from amine capture solution. *Nature Energy* **2021,** *6* (1), 46-53.
14. Li, Y. C.; Lee, G.; Yuan, T.; Wang, Y.; Nam, D.-H.; Wang, Z.; García de Arquer, F. P.; Lum, Y.; Dinh, C.-T.; Voznyy, O., CO2 electroreduction from carbonate electrolyte. *ACS Energy Letters* **2019,** *4* (6), 1427-1431.
15. Kirner, J.; Chen, Y.; Liu, H.; Song, J.; Liao, J.; Li, W.; Zhao, F., Exploring Electrochemical Flow-Cell Designs and Parameters for CO_2 Reduction to Formate under Industrially Relevant Conditions. *Journal of The Electrochemical Society* **2022,** 169, 054511.
16. Lee, J.; Liu, H.; Chen, Y.; Li, W., Bismuth Nanosheets Derived by In Situ Morphology Transformation of Bismuth Oxides for Selective Electrochemical CO2 Reduction to Formate. *ACS Applied Materials & Interfaces* **2022,** *14* (12), 14210-14217.
17. Wu, L.-K.; Wu, W.-Y.; Xia, J.; Cao, H.-Z.; Hou, G.-Y.; Tang, Y.-P.; Zheng, G.-Q., A nanostructured nickel–cobalt alloy with an oxide layer for an efficient oxygen evolution reaction. *Journal of Materials Chemistry A* **2017,** *5* (21), 10669-10677.
18. Duan, Q.; Ge, S.; Wang, C.-Y., Water uptake, ionic conductivity and swelling properties of anion-exchange membrane. *Journal of Power Sources* **2013,** *243*, 773-778.
19. Mahida, B.; Benyounes, H.; Shen, W., Process analysis of pressure-swing distillation for the separation of formic acid–water mixture. *Chemical Papers* **2021,** *75* (2), 599-609.